Verification of spent fuel inside dry storage casks using fast neutrons

Young Ham, Shivakumar Sitaraman, Phil Kerr

Lawrence Livermore National Laboratory
Livermore, CA 94550
Ham4@llnl.gov

Abstract:

Verification of spent nuclear fuel assemblies within dry storage casks has been a major technical challenge for the safeguards regime for decades. Multiple significant quantities of plutonium are present in a single cask, and spent fuel diverted from the dry storage can be potentially used for nuclear weapons or nuclear terrorism. The amount of spent fuel in dry storage casks is rapidly increasing and is expected to triple in one or two decades. Conventionally, spent fuel accountancy in dry storage relies on containment and surveillance approaches, and there are no reliable technical means to re-verify the casks content once a breach in the continuity-of-knowledge occurs or an intrusion is suspected. Application of non-destructive assay methods is significantly limited by close packing of assemblies in storage configuration and extensive shielding that prevent reliable evaluation of gamma-ray and neutron signatures on the periphery of the cask. Although multiple solutions have been investigated in the past, none of them worked properly. This problem remains as the priority for the IAEA Spent Fuel Verification and Monitoring Programs and national regulatory authorities.

The Lawrence Livermore National Laboratory research team has developed a novel approach to address the verification issue of spent fuel in dry storage casks. A modeling and experimental study investigates a spatially-dependent fast- and epi-thermal neutron flux distribution measured at the top surface of the dry storage cask. The neutron intensity pattern is collected over a grid within a specified energy range, resulting in a set of images that characterize the assembly loading configuration. If a gross defect is present (due to an assembly diversion), the neutron map image unambiguously exhibits a strong deviation from the expected distribution. The project is evaluating a number of candidate fast neutron detectors and conducting a parametric design study for a prototype instrument. It is expected that this verification methodology can be adapted to a variety of spent fuel cask configurations: from typical metal/concrete enclosures for above-ground interim storage to metal capsules designated for deep geological disposal.

Keywords: spent nuclear fuel; dry cask storage; fast neutron spectroscopy; stilbene; liquid scintillator

1. Introduction

Spent fuel in dry storage is vulnerable to diversion, and there are currently no technical means to re-verify the contents of dry storage casks, once seals attached to the dry storage casks are damaged or inadvertently removed from a closed cask. The difficulty arises as no useful gamma rays or neutrons from the inner spent fuel seem to penetrate to the outer side surface where measurements can be performed. Multiple studies in the past based on measuring thermal neutrons or gammas have failed to satisfy IAEA requirements [1-3]. Active interrogation methods using conventional external gamma or neutron sources also are impossible to sufficiently detect diversion because they cannot reach the innermost spent fuel assembly. Although cosmic muons can penetrate through the dry storage casks, use of cosmic muons to address the problem would be very challenging in a real world due to its size (difficult to place between dry storage casks), the extremely long data acquisition time (~3 months per one dry storage cask), difficulty in data interpretation, etc. [4]. This problem of re-verification of the integrity of spent fuel inside dry storage has been one of the most technically challenging problems for many decades facing the IAEA as well as other international safeguards communities such as EURATOM or ABACC, and it remains the top priority for the IAEA Spent Fuel Verification and Monitoring Project, one of the top priority R&D needs in the IAEA R&D Plan (T.1.R6), and one of the immediate objectives under Development and Implementation Support Programme for Nuclear Verification 2018-2019 [5,6].

Lawrence Livermore National Laboratory has embarked upon developing a novel methodology for verification of spent fuel inside dry storage casks through detailed modelling. The verification concept to be developed is based upon collecting and analyzing fast/epi-thermal neutrons coming from the top surface of the dry storage casks. When a set of data is collected with an energy selective/sensitive neutron detector on a grid pattern at the top surface of the dry storage cask, the data can produce a neutron image with epi-thermal neutrons or fast neutrons depending upon what type of neutron is used for data acquisition. In the case of diversion of one or more spent fuel assemblies, the neutron image is expected to show deviation from the typical neutron image. Simulated scenarios using MCNP have demonstrated this behavior.

Having collected the neutron signals from the multiple locations above the subject Dry Storage Cask, one does not rely upon a method of using past measurement results, known as the "fingerprinting" method, because the measured profile can show the diversion in a very clear visual manner.

The first part of this report describes the development of a verification concept by modeling a realistic dry storage cask, and performing Monte Carlo radiation transport calculations. The Castor V/21 dry cask that can hold 21 PWR spent fuel assemblies was selected for this purpose. The second part describes laboratory experiments that support the verification concept performed using a Cf252 source and a stilbene fast neutron detector with Castor V/21 measurement geometry.

2. Monte Carlo modeling

Simulations were performed for a limited set of scenarios using the Monte Carlo N-Particle Transport code (MCNP) [7]. Spent fuel neutron and gamma sources were estimated for PWR 17x17 fuel from an operating reactor. Castor V/21 was selected for our modeling study partially for the reason that Castor type casks are widely used throughout the world, and much of its design information was available in the open documents. More than 1,300 Castor type casks have already been loaded and stored in sites all over the world.

2.1 Spent fuel source term evaluation for Monte Carlo Techniques

Source terms for PWR spent fuel assemblies (SFA) were generated with data obtained from discharged fuel from an actual nuclear power plant. Detailed data on the plant operating conditions were obtained in order to obtain realistic source spectra and isotopics.

Pin by pin burnup estimates were available for a few SFAs. Using this information and the average assembly burnup, pin by pin relative burnup levels were calculated. The average pin power can also be calculated using the assembly average power derived from the power plant data.. Based on these two parameters, the average power generated by each pin was determined. The total irradiation time was obtained by combining the pin power, the absolute pin burnup and the mass of heavy metal in each pin.

Using these data, calculations were performed with a general purpose burnup and decay code, ORIGEN-ARP[8], for each specific burnup using the fuel composition based on the initial enrichment of the SFA . Using the pin power consistent with a burnup level, the initial fuel was burned to that level in discrete time steps over the total number of days of the fuel cycle. A run was made to attain each desired burnup level and decayed to obtain spectra in a 47 group structure for neutrons and 20 group structure for gammas at various cooling times. The neutron source terms included contributions from both spontaneous fission and (α, n) events. Neutrons produced by subcritical multiplication were accounted for during the radiation transport process. The isotopics (actinides as well as fission products) consistent with the specific burnup were also obtained for various cooling times. All ORIGEN runs were based on the mass contained in one fuel rod.

SFAs with uniform burnup and real assemblies with non-uniform burnups can be composed using this set of data. In the case of this specific 17x17 SFA, several sets of data were obtained. Given below are two sample sets of data: at 35 GWd/t at 20 years cooling time and 56 GWd/t at 17 years cooling time.

For a spent fuel assembly that is at least 2 years old since its discharge, the neutron source is dominated by spontaneous fission from Cm244 which has a half life of 18.1 years, and to a lesser extent from Pu240 with half life of 6561 years. Although the (α, n) component is one to two orders of magnitude less than the spontaneous fission component, the (α, n) component was still included in the LLNL analyses in the estimation of neutron source. Ignoring the neutron source signal from Cm242 with half-life of only 0.5 years is perfectly acceptable as most of this isotope has decayed away by the time the spent fuel assemblies are transferred into dry storage casks. In the unlikely event that spent fuel less than 2 years old is placed into the dry storage cask, the neutron source from Cm242 cannot be ignored. Thus, the overall spectrum resembles that from a fission source. The normalized spectra at burnups of 56 GWd/t and 35 GWd/t are provided below in Figure 1. The two figures are overlapping.

2.2 MCNP modeling with dry storage cask (CASTOR V/21)

The CASTOR V/21 cask was selected for its wide use, and availability here in US for experimental validation of the proposed verification method. The cask is licensed to contain irradiated 14 x 14, 15 x 15 and 17 x 17 PWR fuel assemblies with Zircaloy fuel rod cladding. Total assemblies allowed per cask is less than or equal to 21. A picture of V21 is shown in Figure 2.

Table 1 shows information and parameters of Castor V/21 used for MCNP modeling. MCNP input information used in the modeling was presented in the form of cross-sectional images of a Castor V/21 DSC that holds 21 17x17 PWR spent fuel assemblies and 21 detectors in Figure 3. One can observe the 290 mm thick primary lid and 90 mm thick secondary lid. Those two lids are dominant shielding material for neutrons coming out of the spent fuel assemblies. In order to optimize computer runtime, 21 detectors with 9.76 cm thick polyethylene (from now on poly in this paper) were placed near the top surface of the DSC. The thickness of the poly was restricted by the need to prevent an overlap with

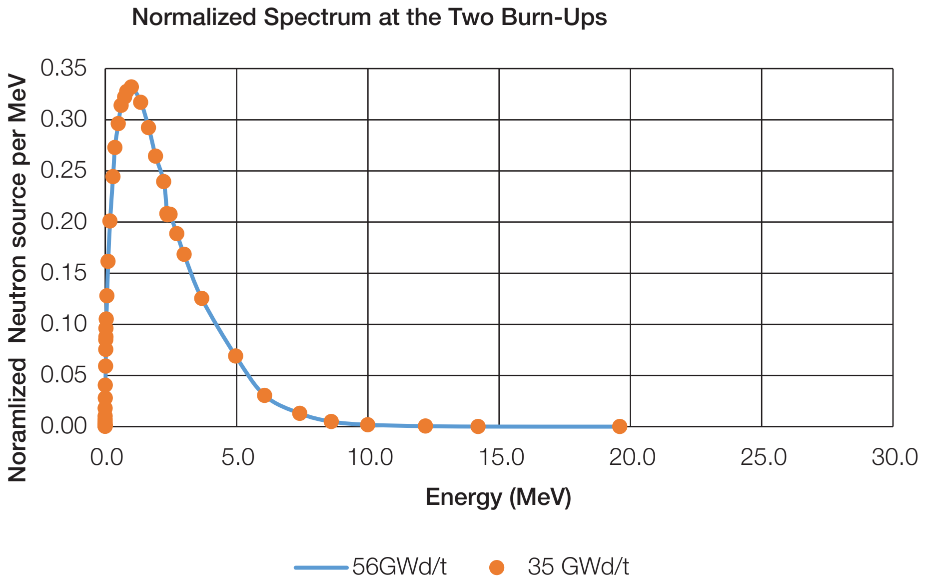

Figure 1: The normalized neutron source spectra used for the MCNP modelling study for both 35 and 56 GWd/t. The two spectra are overlapping.

adjacent detectors in the MCNP model. In actuality this restriction will not apply if only one detector system will be used, allowing the poly thickness to be different. Multiple detectors used simultaneously will obviously have limits on the poly thickness. Every detector was placed directly above the center of the PWR spent fuel assembly. Figure 4 shows a close up view of the axial cross-sectional image in which one can observe fuel rods with plenum region as well as the top nozzles, and the poly (blue region) wrapped detectors (wide black region inside the poly and centered on each SFA).

Figure 2: Picture of Castor V/21 which can accommodate PWR 15x15, 16x16 and 17x17.

Parameter description	Dimension
Overall length of cask	4.866 m (192.4 in)
Cross-sectional diameter of the cask body	2.4 m (94.5 in)
Side wall thickness	37.9 cm (14.9 in)
Length of cask cavity	4.154 m (163.5 in)
Diameter of cask cavity	1.527 m (60.1 in)
PWR spent fuel used	Burnup: 50.76 MWd/kg Cooling time: 17 years
Primary lid thickness	29 cm (11.4 in) stainless steel
Secondary lid thickness	9 cm (3.5 in) stainless steel
Detector cylinder	1 inch radius and 10 cm high
Detector shielding	9.76 cm thick poly
Number of histories in MCNP	$9x10^8$
Variance reductions applied	Source biasing Geometry splitting
Energy bins used for tally	.4 eV, .5 MeV, 1 MeV, 2 MeV, 5 MeV, 10 MeV, 20 MeV

Table 1: Information and parameters of Castor V21 used for MCNP

With MCNP input parameters described above, two cases were studied in order to investigate the proposed concept of using different neutron energy ranges to detect the diversion of a spent fuel assembly. One case was run with the dry storage cask filled with all 21 spent fuel assemblies. Every spent fuel assembly had a burn-up of 56 GWd/t and 17 years of cooling time. Another case was run with the same condition but with the center assembly replaced with a dummy stainless-steel assembly. This means that the detector 2001 (see Figure 5) would be directly above the diverted spent fuel assembly.

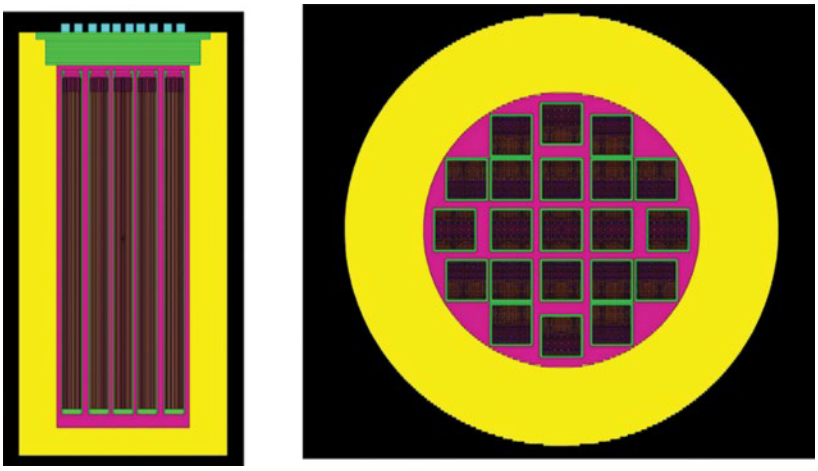

Figure 3: Cut away views of fully loaded CASTOR with 21 17x17 PWR spent fuel assemblies as modeled in MCNP.

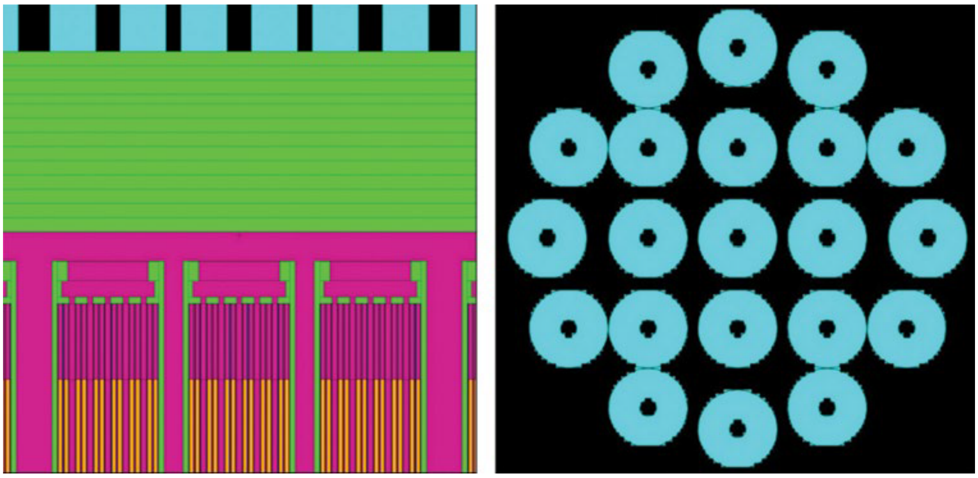

Figure 4: Close up cross-sectional view of MCNP set up. The neutron detectors with poly around them are positioned on the top surface of the CASTOR 21. Every detector is located directly above the center of the PWR spent fuel assembly.

2.3 MCNP Results and Discussions

The MCNP results were tabulated using the format shown in Figure 5 below. The left image indicates the five detectors used to generate the flux profile. The numbers in the right image indicate the number used to designate each detector (tally region) where the flux was calculated. Figure 6 shows the MCNP results in a 2D surface plot. The left plot of Figure 6 is obtained for the case of non-diversion whereas the right plot is for the case of diversion where the center assembly was replaced with a dummy stainless steel assembly. Note that how the center part of the surface plot deviated from the non-diversion case.

Table 2 presents the tally results at the 5 detectors in the center vertical line of the basket (see Figure 5) as a function of neutron energy with all 21 spent fuel assemblies whereas Table 3 presents the results when the center assembly (corresponding to detector 2001) is replaced with a dummy stainless-steel assembly. Figure 7 shows the vertical tally profiles, i.e., detector tally through 2003-2002-2001-2004-2005, as the energy tally bin increases. One can observe a cosine-like shape for the case of no diversion. (The last plot in Figure 7, which corresponds to the tally for the neutron energy 10-20 MeV, did not show a cosine-like shape as the statistical uncertainty for that value was too high. You can find this information in Table 4.) Note how the vertical tally profile obtained with a diversion (orange line) deviates further from the profile with no diversion (blue line) as neutron energy increases. In particular, the profiles with the neutron energies above 1 MeV can visually demonstrate the case of a diversion. This profile method can be a powerful tool as the methodology detects a diversion and it does not require earlier measurement for comparison as in the fingerprinting method.

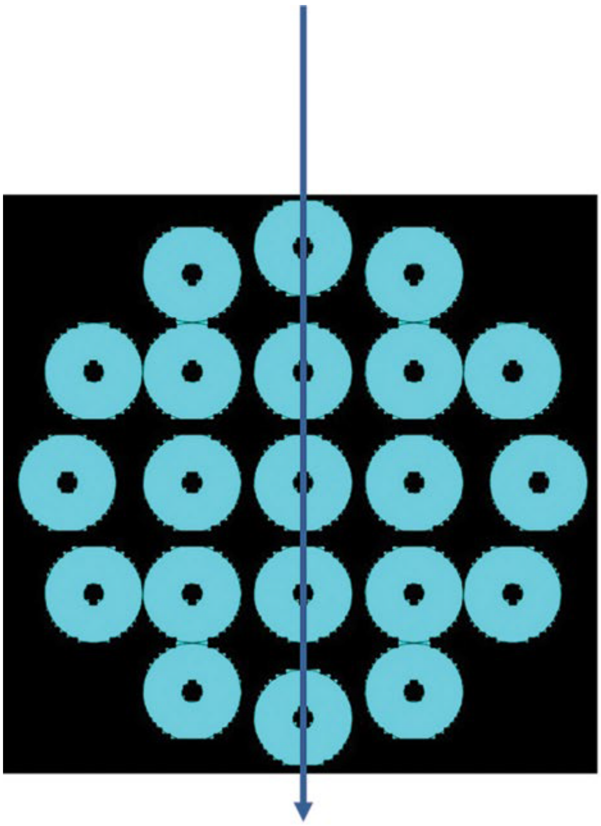

	2014	2003	2011	
2015	2013	2002	2010	2012
2009	2008	2001	2006	2007
2018	2016	2004	2019	2021
	2017	2005	2020	

Figure 5: The left figure indicate how data were read and shown as a graph later for easy analysis and results presentation. The numbers in the right figure indicate neutron tally (detector) number which is essentially relative neutron flux.

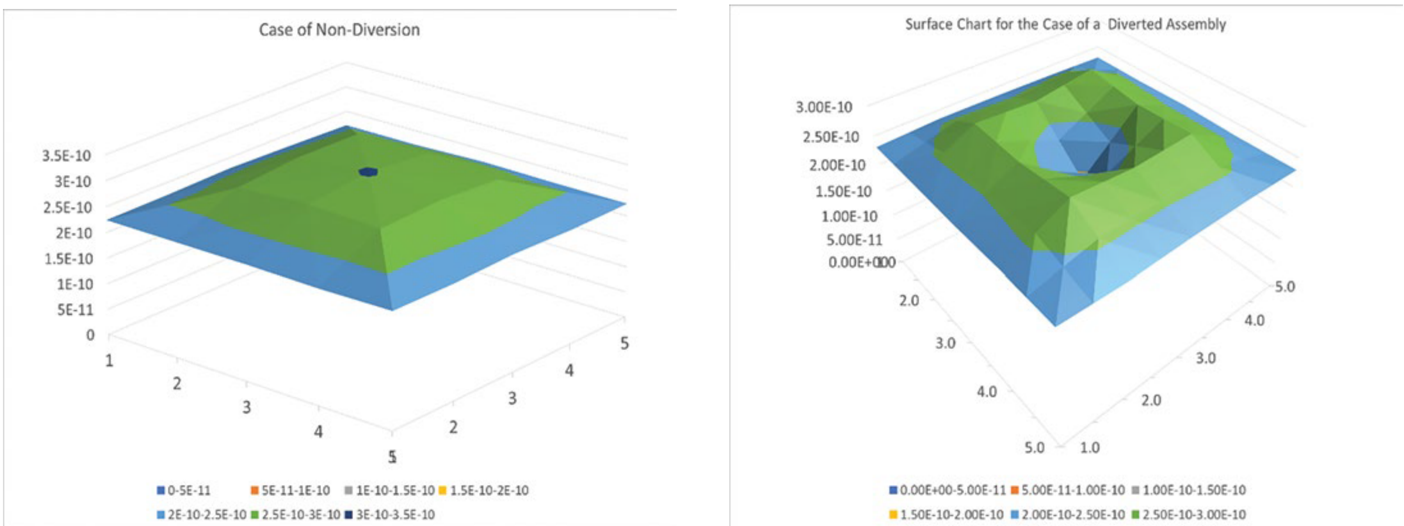

Figure 6: The left figure is obtained for the case of non-diversion. The right figure is for the case where the center assembly was replaced with a dummy stainless steel assembly. Note the deviation in the center in the right figure.

Table 4 shows the neutron tally at the detector 2001 for the case of non-diversion as well as the case with the diversion of an assembly at the center. While the neutron detector tally decreases exponentially with increasing energy, the difference in the flux between the non-diverted and diverted case increases with increasing energy. The amount of deviation, ε, is defined as ε = (neutron tally with no diversion - neutron tally with diversion of an assembly that is subject to verification)/ neutron tally with no diversion

The deviation is a useful quantitative indicator of the diversion of an assembly. The amount of deviation was plotted in terms of neutron energy in Figure 8. For example, if one uses a neutron detector that measures neutron energy in the 2-5 MeV, the relative difference would be 36.4%

It is important to note that the tally used in the MCNP simulation did not account for detector efficiency as the choice of the ideal fast neutron detector to be implemented in the verification tool has not been determined yet.

	Tally (Detector) Data for fully intact assemblies				
Neutron Energy	**2003**	**2002**	**2001**	**2004**	**2005**
0 - 0.4 eV	4.16E-07	5.84E-07	6.29E-07	5.83E-07	4.16E-07
0.4 eV - 0.5 MeV	3.80E-07	5.34E-07	5.75E-07	5.33E-07	3.80E-07
0.5-1 MeV	1.38E-08	1.96E-08	2.10E-08	1.95E-08	1.37E-08
1-2 MeV	1.92E-09	2.65E-09	2.76E-09	2.64E-09	1.92E-09
2-5 MeV	2.24E-10	2.88E-10	3.02E-10	2.92E-10	2.26E-10
5-10 MeV	3.05E-11	3.85E-11	3.95E-11	3.83E-11	3.07E-11
10-20 MeV	1.74E-12	2.00E-12	2.14E-12	2.34E-12	1.93E-12
Total	8.12E-07	1.14E-06	1.23E-06	1.14E-06	8.11E-07

Table 2: Tally at vertical center 5 detectors as a function of neutron energy with full intact assemblies.

	Tally (Detector) Number for missing central assembly (2001				
Neutron Energy	**2003**	**2002**	**2001**	**2004**	**2005**
0 - 0.4 eV	4.18E-07	5.74E-07	6.06E-07	5.74E-07	4.18E-07
0.4 eV - 0.5 MeV	3.82E-07	5.25E-07	5.53E-07	5.24E-07	3.82E-07
0.5-1 MeV	1.40E-08	1.89E-08	1.88E-08	1.89E-08	1.38E-08
1-2 MeV	1.97E-09	2.56E-09	2.21E-09	2.52E-09	1.96E-09
2-5 MeV	2.30E-10	2.75E-10	1.92E-10	2.76E-10	2.31E-10
5-10 MeV	3.09E-11	3.55E-11	2.36E-11	3.82E-11	3.12E-11
10-20 MeV	1.52E-12	2.28E-12	1.28E-12	2.29E-12	1.92E-12
Total	8.16E-07	1.12E-06	1.18E-06	1.12E-06	8.16E-07

Table 3: Tally at vertical center 5 detectors as a function of neutron energy with the center assembly replaced with a dummy stainless-steel assembly.

Cell	2001 (Full)		2001 (Diverted)		Deviation (ε)
Neutron Energy (MeV)	**Tally**	**Error**	**Tally**	**Error**	
0 - 0.4 eV	6.29E-07	0.07%	6.06E-07	0.07%	**3.66%**
0.4 eV - 0.5	5.75E-07	0.07%	5.53E-07	0.08%	**3.83%**
0.5-1	2.10E-08	0.24%	1.88E-08	0.25%	**10.5%**
1-2	2.76E-09	0.55%	2.21E-09	0.76%	**19.9%**
2-5	3.02E-10	0.89%	1.92E-10	1.21%	**36.4%**
5-10	3.95E-11	2.12%	2.36E-11	3.13%	**40.3%**
10-20	2.14E-12	8.55%	1.28E-12	14.24%	**40.2%**
Total	1.23E-06	0.07%	1.18E-06	0.07%	**3.90%**

Table 4: Neutron intensity, the tally at detector 2001, for the case of non-diversion and the case with the diversion of an assembly at the center. Relative difference can be interpreted as deviation.

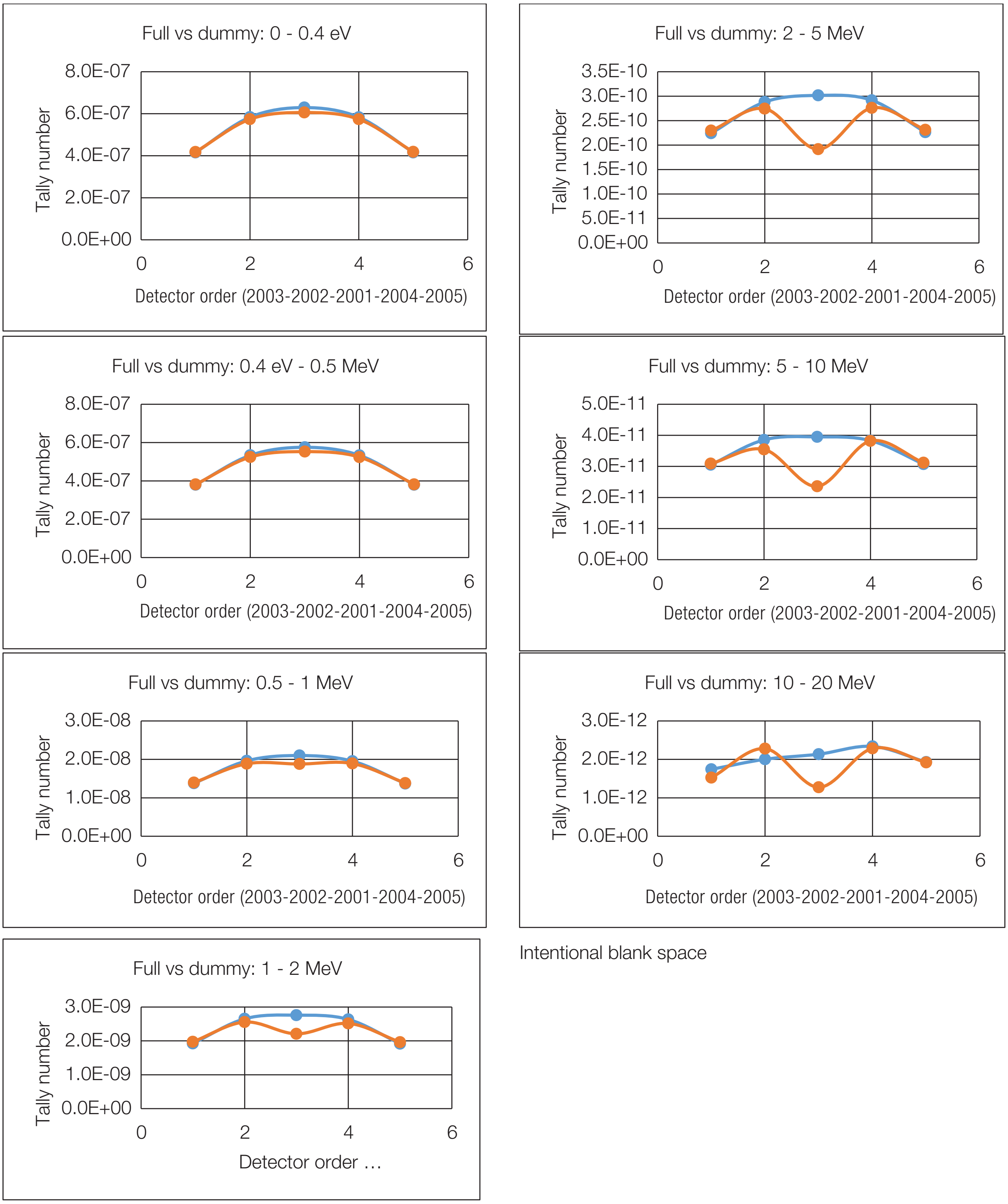

Figure 7: Vertical tally profiles, i.e., detector tally through 2003-2002-2001-2004-2005, as the energy tally bin increases.- The blue curve is the cask with all 21 assemblies and the orange curve is when the center assembly has been replaced with a stainless steel dummy assembly.

3. Experiments

An experiment was set up in the laboratory to validate the verification concept as a precursor before doing actual validation measurements at a dry storage cask site. The measurement geometry was arranged to mimic the data acquisition for the dry storage measurement environment (see Figure 9.) For the experiments, a stilbene detector, was selected as one of the several fast neutron detectors to be studied, to obtain fast neutron signals due to their high efficiency, commercial availability in large sizes, and good characterization of gamma discrimination by use of pulse shape discrimination (PSD). As stilbene is known to be very responsive to gamma rays, PSD application to the measured data is critically important to assess neutron signals. The PSD method is based on the difference in the decay time of fluorescence emitted within an organic scintillator as a result of a reaction between the ionizing particle and the scintillator. The fluorescence decay time for heavy particles, such as protons, or neutrons is much longer than that of electrons.

The data acquisition system, shown in figure 9, consists of a Fast Comtec MPA-3 four channel muliparameter system, and a Mesytec MPD-4 pulse shape discriminator unit. The MPD-4 unit examines the time structure of the electrical pulse from the PMT to discriminate between neutrons and gamma rays that interact with the stilbene scintillator.

As shown in Figure 9, a 4-inch diameter, 2-inch deep stilbene was used to collect one set of data when the Cf252 was placed directly below the detector in the center of the collimator space (position 1), and another set of data when the Cf252 placed at the off-collimator position (position 2). The detector was placed at 8.5 cm above the top surface of the

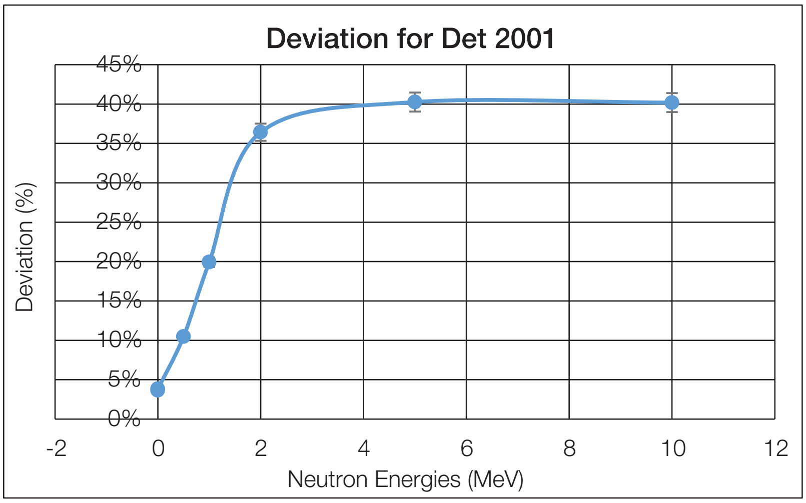

Figure 8: Deviation for detector 2001 in terms of neutron energy. Note how the deviation increases rapidly as neutron energy increases. Here deviation shows the degree of deviation from the case of non-diversion.

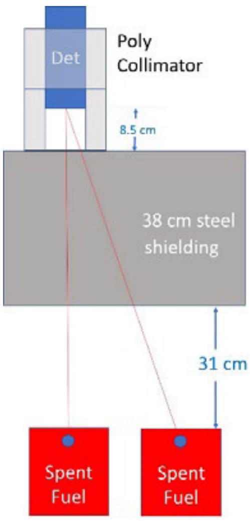

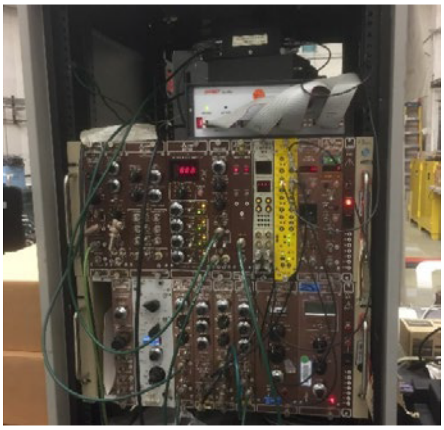

Figure 9: Experimental set up and data acquisition electronics. The two red boxes indicate the position and dimension of spent fuel assemblies in the dry storage casks in scale, although no spent fuel was used in the actual measurements. The two blue circles represent the Cf source position. The picture on the right shows the Fast Comtec MPA-3 four channel multiparameter system on the top, and a Mesytec MPD-4 pulse shape discriminator unit in the NIM bins.

steel inside the cavity of a poly collimator. Each set of data was collected over a measurement time of 1 day. The distance between the two Cf252 source positions was set to be at 27.75 cm representing actual pitch of two adjacent SFAs on the center line of two SFAs as stored in the Castor cask.

4. Results and data analysis

PSD plots obtained with the stilbene scintillator using PSD electronics for the case of a Cf252 source placed directly below the detector and the source at the off-collimator position are shown in Figure 10. The neutron signals were attenuated by 38 cm of steel which is the thickness of the Castor V/21 lids. The upper neutron band signals were well separated from the lower gamma band signals.

Note that in the PSD plots in Figure 10, the neutron signal bands contain energy information, but they do not represent the direct neutron energy information. Thus, the PSD plots cannot be treated as neutron energy spectra requiring unfolding of the PSD plots. As the process of unfolding spectra requires substantial effort and is perhaps cumbersome to apply for verification, a method was explored for the PSD plots to be directly applicable for verification. As our verification methodology requires information on the energy of neutrons that come into the detector, particularly, the energy threshold of 1 MeV or 2 MeV in the measured spectra produced by poly-energetic neutron source, i.e. spent fuel, an effective neutron calibration method is needed. One approach that was adopted is making use of a D-D neutron generator knowing that it produces near monoenergetic neutrons at approximately 2.4 MeV.

The left plot in Figure 11 shows the PSD plot produced by stilbene with the use of a D-D 2.4 MeV neutron generator. Observe a distinctive end of neutron band that ends in near channel 170, a feature that can be useful to separate

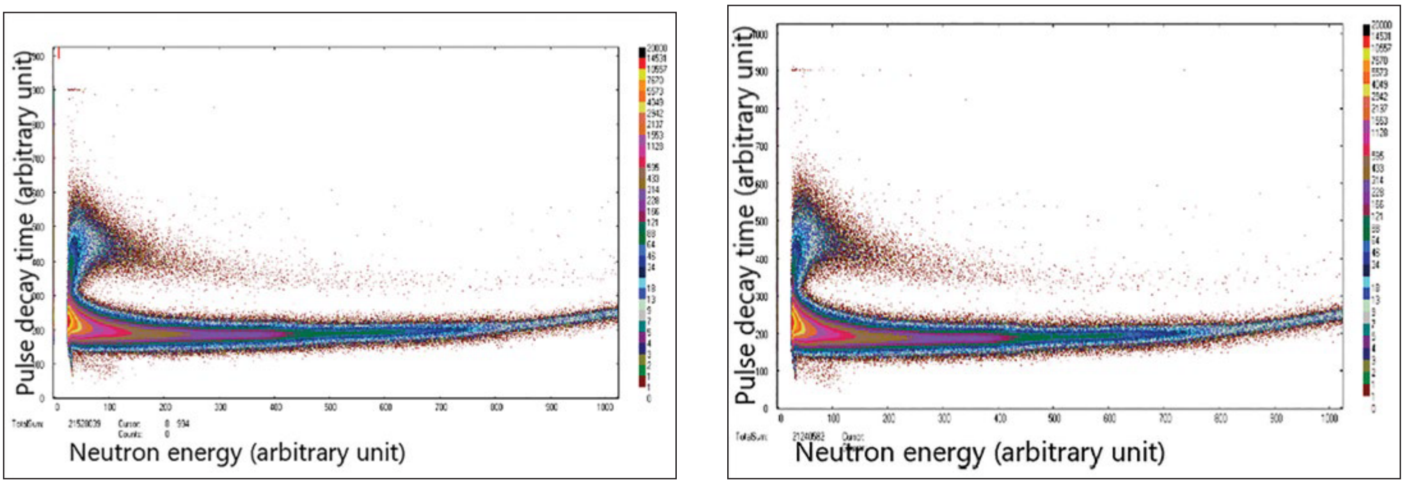

Figure 10: PSD plots obtained with the stilbene scintillator using PSD electronics for the case of Cf source placed directly below the detector and the source off the collimator position. The radiations were attenuated by 38 cm of steel. The upper neutron band signals were well separated from the lower gamma band signals.

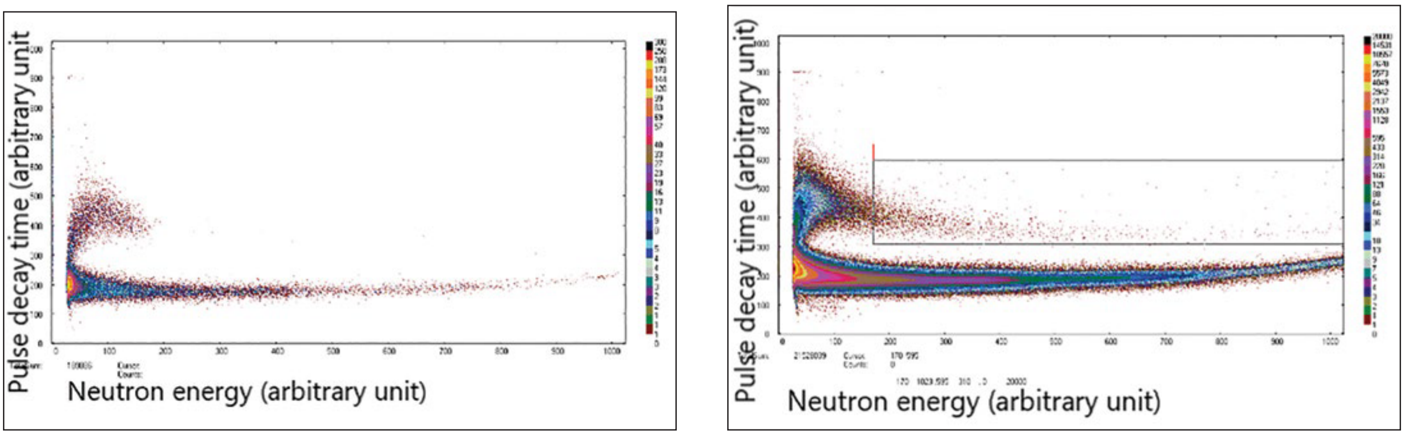

Figure 11: PSD plot in the left obtained with the stilbene scintillator using PSD electronics and DD 2.4 MeV neutrons. Note that there is a distinctive end of neutron band, showing a feature that can be useful to separate neutron signals. The information is used to select a rectangular ROI that predominantly has neutrons with energy greater than approximately 2.4 MeV. An example of ROI selection is shown in the right plot.

neutron signals below 2.4 MeV for the data obtained with poly-energetic neutron source such as Cf252 or spent fuel. Using this piece of information, the region of interest (ROI) was selected to capture neutrons above 2.4 MeV from the PSD plots obtained at two source positions (see the right plot in Figure 11.)

The neutron counts in the ROIs were found to be 8051 +/- 1.2% and 5753 +/- 1.3% with background subtraction respectively for source position 1 (on collimator axis) and position 2 (off collimator axis). This corresponds to a difference in neutron signals by 27.7%. The amount of deviation in the actual V/21 arrangement is difficult to estimate with this value alone as all assemblies contribute to the total counting, and due to the difference in source geometry and source strength between Cf252 and actual spent fuel assemblies. However, substantially measurable difference in the neutron strength is expected in the case of a diversion of an entire assembly. The experimental result will be improved by selecting a smaller diameter stilbene, a thicker collimator and the optimal position of the detector. Further experiments are in progress.

The results obtained in these experiments showed that verification of spent fuel inside dry storage casks is possible by use of stilbene and a simple 2.4 MeV energy threshold method. The results are also consistent with MCNP modeling results, although a direct comparison of the experimental results with the MCNP modeling results was not possible due to different geometry and the inability of using actual spent fuel in the experiments in the lab environment. Besides the stilbene, several different types of fast neutron detectors are also being explored as a potential fast neutron detector to be a part of the verification system for spent fuel in dry storage casks. Preliminary data using a liquid scintillator, EJ-309, showed similar results as those from the stilbene detector.

5. Conclusions

A novel methodology was proposed and validated by simulation and laboratory experiments to address the long unsolved technical problem of verification of spent fuel inside dry storage casks. The verification concept uses an energy selective neutron detector measuring neutron signals on a grid pattern at the top surface of the dry storage cask. In the case of diversion of one or more spent fuel assemblies, the neutron image is expected to show a deviation from the typical neutron image. The verification method is intuitive, easy to interpret, and does not rely upon any past measurement results. Simulated scenarios using MCNP have demonstrated this capability. Simplified laboratory experimental results using Cf252 and a stilbene scintillator showed that the proposed methodology is indeed very promising.

6. Acknowledgements

This work was sponsored by the US Department of Energy, National Nuclear Security Administration, Office of Nonproliferation and Arms Control, International Nuclear Safeguards program, and performed under the auspices of the US Department of Energy by Lawrence Livermore National Laboratory under Contract DE-AC52-07NA27344.

7. References

[1] Ziock, K., Vanier, P., Forman, L., Caffrey, G., Wharton, J. and Lebrun, A., 'The feasibility of cask "fingerprinting" as a spent-fuel, dry-storage cask safeguards technique', UCRL-TR-215943, 2005.

[2] Jayson Wharton, C., Seabury, E. H., Caffrey, A. J. and Winston, P. L., *Summary Report: INL CDCIS cask scanner testing at Doel, Belgium,* 2013.

[3] Santi, P. A., Browne, M. C., Freeman, C. R., Parker, R. F. and Williams, R. B., 'Initial measurement of BN-350 spent fuel in dry storage casks using the dual slab verification detector', LA-UR-10-03849, 51st INMM Annual Meeting, Baltimore MD, 2010.

[4] Durham, J. M., Poulson, D., Bacon, J., Chichester, D. L., Guardincerri, E., Morris, C. L., Plaud-Ramos, K., Schwendiman, W., Tolman, J. D. and Winston, P., 'Verification of spent nuclear fuel in sealed dry storage casks via measurements of cosmic-ray muon scattering', *Physical Review Applied*, Vol. 9, No 4, 044013, 2018.

[5] International Atomic Energy Agency, STR-385, *Research and Development Plan*, Vienna, 2018.

[6] International Atomic Energy Agency, STR-386, *Development and Implementation Support Programme for Nuclear Verification 2018-2019,* Vienna, 2018.

[7] Werner, C. J. (ed.), *MCNP Users Manual — Code Version 6.2*, Los Alamos National Laboratory, 2017.

[8] Reardon, B. T. and Jeesee, M. A. (eds), *Scale Code System, Version 6.2.3, ORNL/TM-2005/39,* Oakridge National Laboratory, 2018.